GENERATIVE ATLASES AND ATLAS SELECTION FOR C11-PIB PET-PET REGISTRATION OF ELDERLY, MILD COGNITIVE IMPAIRED AND ALZHEIMER DISEASE PATIENTS

J. Fripp[1], P. Bourgeat[1], O. Acosta[1], G. Jones[3], V. Villemagne[3], S. Ourselin[1,2], C. Rowe[3], O. Salvado[1]

The Australian e-Health Research Centre, CSIRO ICT Centre, Brisbane, Australia.
[2] Centre for Medical Image Computing, University College London, UK.
[3]Department of Nuclear Medicine and Centre for PET, Austin Hospital, Australia

ABSTRACT

$\beta - amyloid$ (Aβ) plaques are one of the neuropathological hallmarks of Alzheimer's disease (AD) and can be quantified using the marker ^{11}C PiB. The registration of ^{11}C PIB PET images to an atlas allows spatial normalization and statistical comparisons. This generally involves a co-registration of the PET and MR which is then registered to an MR atlas. The use of PET to PET atlas registration is much less common, although important as MR scans are not always available. In this paper we present a study on using PET to PET atlas registration with the corresponding MR registration used as the reference standard. Average affine and non-rigidly aligned PET Atlases were created, as well as a principal component based generative atlases. From this work we found that the use of multiple registrations to a generative affine ^{11}C PIB PET atlas obtains the best results, with a mean translation error of 1.67 mm, and average point to point error around the cortex of 2.77 mm. As the obtained results are almost the same as using PET-MR co-registration and propagation to an atlas, and in some cases qualitatively they can appear better, we believe this may be a suitable approach for ^{11}C PIB PET registration, which may avoid the need for acquiring the MR and performing multimodality registration.

***Index Terms*—** PET, atlas generation, registration

1. INTRODUCTION

$\beta - amyloid$ (Aβ) plaques are one of the neuropathological hallmarks of Alzheimer's disease (AD) and appear many years before cognitive symptoms become apparent. ^{11}C PIB PET [1] is one of the most promising imaging agents for assessing Aβ deposition. In previous studies, it has been observed that the pattern of uptake found in ^{11}C PIB PET images can vary significantly and in some cases overlaps between AD, mild cognitive impaired (MCI) and normal elderly controls (NC). Some example ^{11}C PET images are presented in Fig. 1, which highlight the variability observed.

The variation in brain structure and Amyloid deposition between individuals and differences in image resolution and field of view can make direct comparisons of ^{11}C PIB PET images difficult. To perform statistical analysis some form of standardization is essential. It is believed that the cerebellar grey matter is devoid of receptors and only contains diffuse Aβ plaques which PIB binds to non specifically. As such the cerebellum is often used as the reference region to determine the standard uptake value ratio (SUVR), which can then be used to normalized the intensity of the image. The standard approach to perform spatial normalization is through linear scaling and non-linear warping, which is often performed using the SPM software for example [2]. For this the patients ^{11}C PIB PET and MR
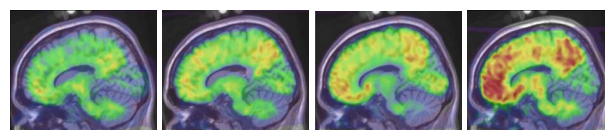

Fig. 1. Three example cases of ^{11}C PIB PET overlaid on the Colin atlas *left* Healthy elderly *middle left* mild cognitive impaired *middle and far right* Alzheimer's. **Note:** These are obtained by co-registering the subjects ^{11}C PIB PET and MR images, the subjects MR is then affinely and non-rigidly warped to the Colin atlas, with the obtained transforms applied to the subjects ^{11}C PIB PET image.

are co-registered. The patients MR is then affinely and non-rigidly warped to an atlas, with the warping applied to the ^{11}C PIB PET to obtain spatially normalized images [3, 4]. The primary disadvantages of this is that there is an accumulation of registration errors and it requires an MR to be acquired for each patient.

In FDG PET studies and in some PIB studies an average PET atlas has been used [5]. However, to our knowledge there has been little work performed in quantifying the accuracy of this, especially for ^{11}C PIB PET images, which exhibit a highly variable tracer uptake with significantly less relationship to the underlying anatomy than FDG. This variability indicates that the use of a single average atlas for ^{11}C PIB PET registration may not be optimal and may even bias registration results and errors.

In this paper we investigate whether it is possible to perform ^{11}C PIB PET-PET affine image registration without a significant loss of accuracy compared to performing co-registered ^{11}C PIB PET-MR and MR to Atlas affine registration. For this work we compare several strategies to perform affine registration and present the use of a generative ^{11}C PIB PET atlas to allow more accurate PET only affine registration.

2. METHODOLOGY

2.1. Subjects

PiB PET scans from 58 participants enrolled in a longitudinal study assessing the usefulness of ^{11}C PiB PET for early diagnosis of AD were used in this study [6]. Participants were excluded if they were not fluent in English, mini-mental state examination (MMSE) was less than 12, or there was a history of brain injury or alcoholism. The 24 AD participants met NINCDS/ADRDA criteria for probable AD. The 20 MCI participants met Petersen's recently published consensus criteria. The remaining 54 participants were healthy elderly participants. Objective impairment was established as at least one

neuropsychological test score falling 1.5 SD or more below relevant normative data.

2.2. Image Acquisition Protocols

The ^{11}C PiB PET scans were acquired using a Philips ADAC Allegro full-ring tomograph with PIZELAR germanium oxyorthosilicate crystal detectors. Each participant was injected with 370 MBq of ^{11}C-PiB and were scanned for 20 minutes starting 40 minutes post-injection. Summed images for the 40 to 60 minutes time frame were used in this study (2x2x2mm). Sagittal MR images were acquired using a T$_1$ weighted 3D SPGR sequence 1.5T (1.1x1.1x1.5mm) and 3T scanners (0.5x0.5x2mm).

2.3. Registration

In this paper we keep the registration scheme fixed and consider the choice and influence of target (atlas) selection on registration accuracy. The image registration was performed using the automated method of Ourselin et al [7], which has been previously validated using the Vanderbilt database. This approach uses a block matching strategy to estimate the transformation by extracting small blocks in the two images to be registered and iterating the following steps until convergence:

- Pair each image block of the PET image with the closest image block in the MR image

- Compute the transformation that will best match the paired blocks

- Apply this transformation to the feature points of the PET image.

The pairings were updated at each iterations after applying the transformation. A total of 5 iterations of these three steps were used to obtain an optimal match. The matching criteria used was normalized cross-cross correlation.

2.4. Atlases and generative atlas

For this work we used five different atlases (Fig. 2), the Colin atlas, average affinely and non-rigidly registered ^{11}C PIB PET images, and an affine and non-rigid versions of the generative atlas. The Colin and average atlases had 1mm isotropic spacing, while the generative atlas was resampled to 2mm isotropic spacing.

All subject's co-registered MR scans were spatially normalized to the Colin atlas [8]. Non-rigid spatial normalization was performed using the aforementioned affine registration [7] and a B-Spline based free form deformation (FFD) algorithm [9]. The matching criteria used in the FFD was normalized mutual information (NMI) [10]. The obtained transformations were then used on the subjects ^{11}C PIB PET image to spatially normalize it to the Colin atlas. The ^{11}C PIB PET images were not standard uptake value normalized, instead a zero mean, unit variance intensity normalization was performed. The filtered images were then used to create average and generative atlases. The images used in the generative atlas were downsampled from the 1 mm spacing of Colin to 2mm spacing seen in the original PET images.

Given N images with $M = N_x N_y N_z$ samples we can construct a $X = M \times N$ matrix (each column i is the voxel data from the i th image x_i). Then the mean image is simply $\mu = \frac{1}{N}\sum_{i=1:N} x_i$. The principal component model was calculated using a singular value

decomposition (SVD) with the covariance matrix $\frac{1}{N}DD^T$ decomposed as $U\sum U^T = \frac{1}{N}DD^T$ where D is the mean-offset map (column i given by $D_i = x_i - \mu$), and U has column vectors that represent the orthogonal modes of variation and $\sum$ is a diagonal matrix of corresponding eigenvalues. An image x_{unseen} can be decomposed into a N dimensional vector of weights $w = U^T(x_{unseen} - \mu)$, which we'll refer to as eigen-weights. Given eigen-weights w, an image x_{new} can be reconstructed by $x_{new} = Uw + \mu$. This model was used to generate atlas cases.
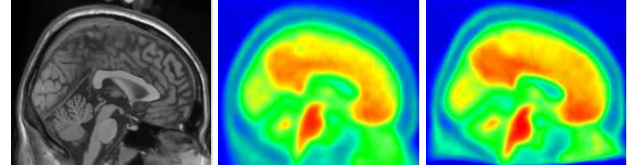

Fig. 2. Example slices from the *left* Colin Atlas *middle* Average affinely registered ^{11}C PIB PET *right* average non-rigid registered ^{11}C PIB PET image

2.5. Registration Experiments

The registration of ^{11}C PIB PET images was performed using 6 different schemes, so we obtain 6 different affine transforms for each patient. The different approaches are presented schematically in Fig. 3. The first scheme was used as the reference standard and involved the rigid co-registration of the PET and MR which was then affinely registered to the Colin atlas. The second approach directly affinely registers the PET to the Colin atlas. The third (and fourth) approach registers the PET to the average affinely (and non-rigidly) registered ^{11}C PIB PET image.

The fifth and sixth schemes were iterative and initialized using the average image. The atlas used at each iteration was generated using the weights obtained by decomposing the transformed PET image (from the previous iteration) with the principal component model (Fig. 4). As a result of this the atlas iteratively evolves to look more like the PET case. So for an AD case it will become more AD like, while a healthy elderly case will become more NC like.
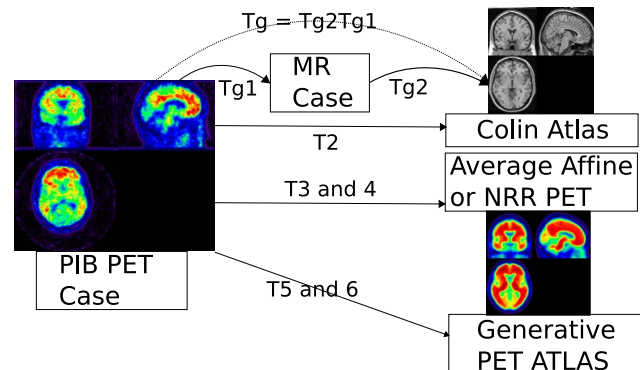

Fig. 3. Summary of the atlases used in registering the ^{11}C PIB PET images. **Note:** T_{g1} is a rigid transformation, while all others are affine.

Ti

PIB PET

PET ATLAS (i-1)

T(i-1)(PIB PET)

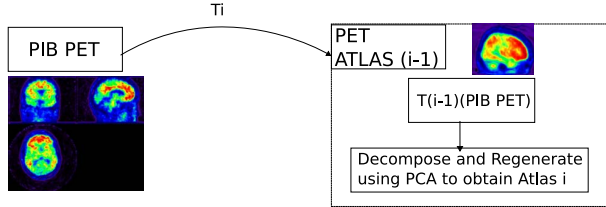Decompose and Regenerate using PCA to obtain Atlas i

Fig. 4. Brief overview of the use of the generative atlas. At iteration $i = 0$ the ^{11}C PIB PET image is registered to the mean atlas created by the voxel based principal component (PC) analysis. After registration, the ^{11}C PIB PET image is projected into the PC model to extract the eigen-weights, which are constrained to 3 standard deviations. These eigenweights are then used to generate the atlas image for the subsequent iterations.

2.6. Validation

To validate the accuracy of the registration we extract a surface mesh of the cortex from the AAL template and propagated this back onto the PET images using the obtained affine transforms. With the coregister PET to MR to Atlas being used as the reference standard, the error in the centroid distance and point to point distances are calculated for each approach.

To analyze the resulting affine transform M we decompose it using a polar decomposition [11] so that $M = QS + T$. The Q matrix is pure rotation, S consists of scale and skew and T is the translation. The versor components are then extracted from the Q matrix. The transform decomposition obtained from the co-registration of the PET to the MR, and MR to the Colin atlas is combined and used as the standard. The transform decompositions obtained using the other approaches were then compared with this.

It should also be noted that the generative atlas was created and used in a leave one out strategy.

3. RESULTS AND DISCUSSION

All approaches were found to obtain fairly similar results, with an accuracy that was similar to the voxel size of the PET image (Table 1). As can be seen in Table 1 only a small fraction of the cases failed (error more than 3 mm). It can be clearly seen that the use of affine generative atlas obtained the best overall results. This is particularly good considering the generative atlas was resampled to half the resolution of the other atlases. For this work three iterations of the generative atlas were used, at which time the registration and atlas generation had essentially converged. Fig. 5 and Table 1 presents an overall summary of the results of propagating the cortex surface back into PET space and comparing these to the propagated reference surface. The average surface point to point error on the cortex was fairly small, especially if one considers small errors in rotation. The overall error in the rotation is presented in Table 2.

Fig. 6 illustrates that it sometimes appears that the results obtained by the generative atlas may be preferable to our reference standard. This is interesting to consider, especially when one observes the small differences in the neocortex boundaries that are evident on the surface renderings (Fig. 7). In this case the cause of the errors in Fig. 6 appear to be from the PET-MR co-registration, with a section of skull poorly aligning. These small errors in multimodality registrations are often observed and are hard to avoid. However, as

Table 1. Average (Std) measures for all the cases in the database

Atlas	Centroid Err (CE)	P2P Err	# CE > 3mm
PET to Colin	1.99 (0.98)	3.18 (1.34)	6
PET to Affine	1.82 (0.91)	2.78 (0.83)	8
PET toGenAffine	1.67 (0.79)	2.77 (0.80)	4
PET to NRR	2.16 (1.00)	3.08 (0.87)	8
PET toGenNRR	1.77 (0.80)	3.01 (0.83)	6

Table 2. Average sum of square distance for the three versor angles

Atlas	Mean Error (Std)	Median error
Pet to Colin	0.0217 (0.0134)	0.0134
Pet to Affine	0.0143 (0.0068)	0.0126
Pet to Generative Affine	0.0176 (0.0085)	0.0163
Pet to NRR	0.0152 (0.0074)	0.0137
Pet to Generative NRR	0.0196 (0.0090)	0.0191

we have no ground truth we haven't yet investigated this properly. In the future we hope to be able to quantitatively compare the results obtained by the generative atlas and our current reference standard.
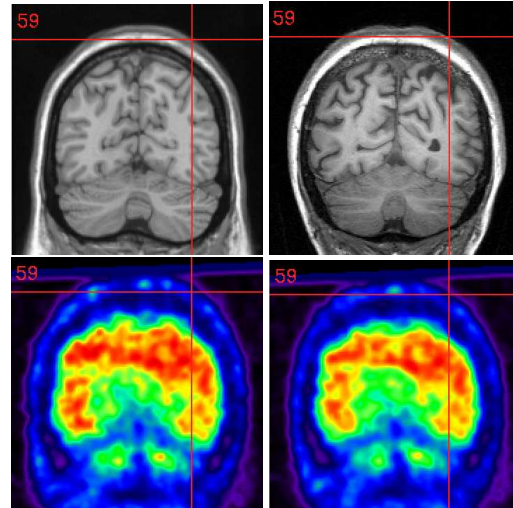

Fig. 6. Observed error on the skull in the co-register and propagated (bottom right) PET image, *top left* Colin Atlas *top right* MR registered to Colin *bottom left* PET propagated to Colin *bottom right* PET registered to Generative atlas

4. CONCLUSION

In this paper we have presented a comparison of several different ways of registering ^{11}C PIB PET images to an atlas. In this work we found that the best results for ^{11}C PIB PET registration (without MR information) was obtained by using a generative affine ^{11}C PIB PET atlas. The ground truth for this work was the results of a PET-MR coregistration and propagation to an atlas. The PET resolution and the generative atlas are 2 mm isotropic resolution, so obtaining
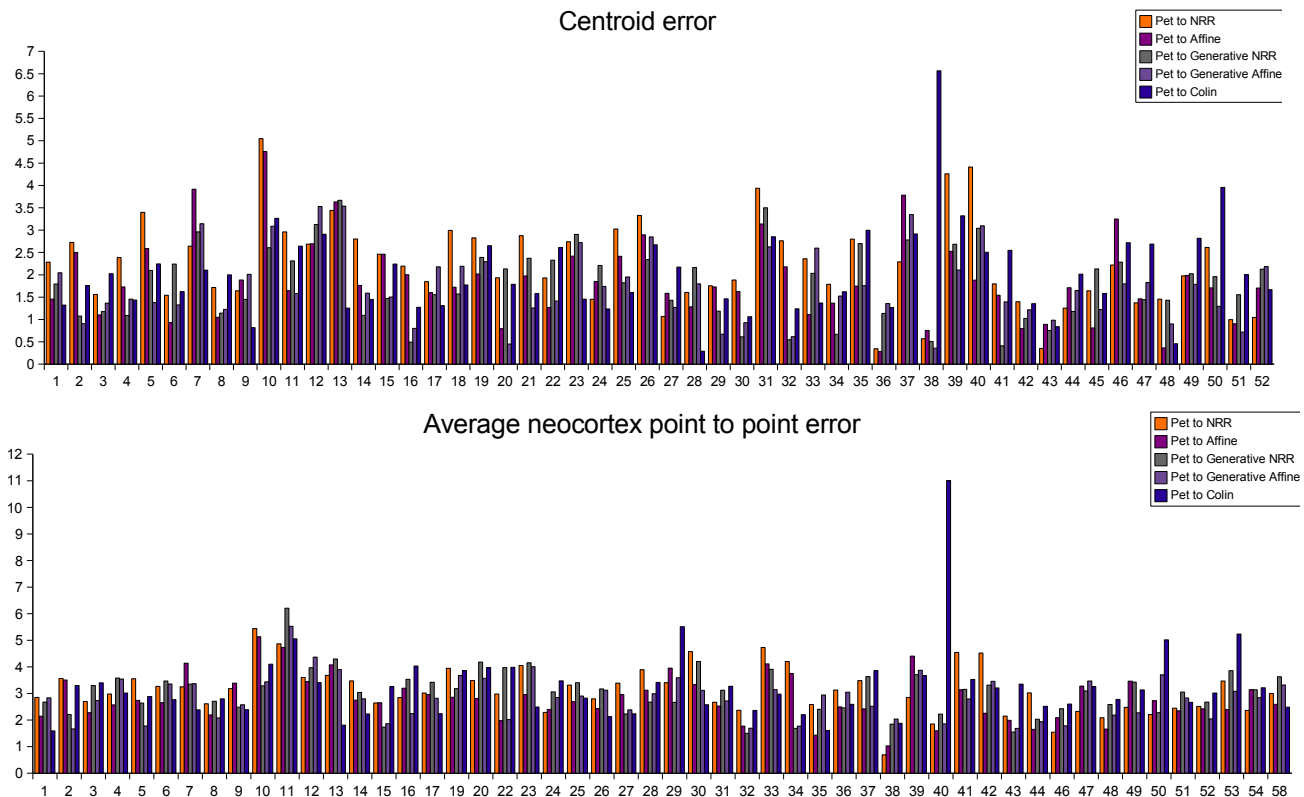
Fig. 5. *top* Error in centroid for each case *bottom* Average error in point to point measure on cortex for each case
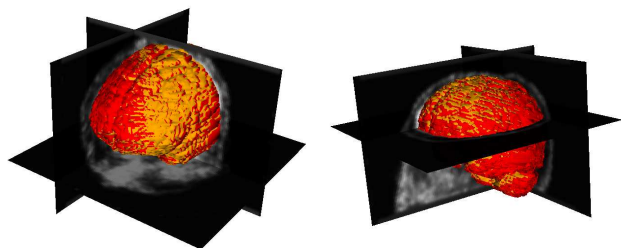

Fig. 7. Surface renderings of propagated neocortex surface for two cases, with the gold surface is the reference and the red obtained by the generative atlas. The generative surface is generally slightly larger than the reference.

an average translation error of only 1.67 mm, and average point to point error around the cortex of 2.77 mm seems reasonable. This approach was also the most robust with only 4 of the 58 cases having a centroid error of more than 3 mm. The primary disadvantage of this approach is the increase in computation time required (linear with number of generative atlas iterations). Future work involves further validation of these results, especially the multimodality coregistrations and investigation into the use of normalized mutual information. It is also believed that this could be extended to use non-rigid registration algorithms which allow high dimensional warping, by imposing deformation constraints.

5. REFERENCES

[1] W E Klunk, H Engler, and *et al.*, "Imaging brain amyloid in Alzheimer's disease with Pittsburgh Compound-B," *Ann Neurol*, vol. 55, no. 3, pp. 306–319, Mar. 2004.

[2] J. Ashburner and K.J. Friston, ""Nonlinear Spatian Normalizatioon Using Bbasis Functions"," *in Human Brain Mapping*, vol. 7, pp. 254–266, 1999.

[3] S.K. Ziolko and L.A. Weissfeld *et al*, "Evaluation of voxel-based methods for the statistical analysis of PIB PET amyloid imaging studies in Alzheimer's disease," *Neuroimage*, vol. 33, no. 1, pp. 94–102, Oct 2006.

[4] B.J. Lopresti and W.E. Klunk *et al*, "Simplified quantification of Pittsburgh Compound B amyloid imaging PET studies: a comparative analysis," *J Nucl Med*, vol. 46, no. 12, pp. 1959–1972, Dec 2005.

[5] S.K. Lee, S.S. Lee, J.A. Yeo, J.A. Lee, Y.K. Kim, M.J. Jang, K.K Kim, S.K. Kim, J.B. Oh, and C.K Chung, "Fdg-pet images quantified by probabilistic atlas of brain and surgical prognosis of temporal lobe epilepsy," *Epilepsia*, , no. 9, pp. 1032–1038, Sep 2002.

[6] C C Rowe, S Ng, U Ackermann, S J Gong, K Pike, G Savage, T F Cowie, K L Dickinson, P Maruff, D Darby, C Smith, M Woodward, J Merory, H Tochon-Danguy, G O'Keefe, W E Klunk, C A Mathis, J C Price, C L Masters, and V L Villemagne, "Imaging beta-amyloid burden in aging and dementia," *Neurology*, vol. 68, no. 20, pp. 1718–1725, May 2007.

[7] S. Ourselin and A. Roche *et al*, "Reconstructing a 3D structure from serial histological sections," *IVC*, vol. 19, pp. 25–31, 2001.

[8] D.L. Collins, A.P. Zijdenbos, V. Kollokian, J.G. Sled, N.J. Kabani, C.J. Holmes, and A.C. Evans, "Design and construction of a realistic digital brain phantom," *IEEE Transactions on Medical Imaging*, vol. 17, no. 3, pp. 463–468, June 1998.

[9] D. Rueckert, L.I. Sonoda, C. Hayes, D.L.G. Hill, M.O. Leach, and D.J. Hawkes, "Nonrigid registration using free-form deformations: Application to breast mr images," *in IEEE Trans. Med. Imag.*, vol. 18, pp. 712–721, August 1999.

[10] C. Studholme, D.L.G. Hill, and D.J Hawkes, "An Overlap Invariant Entropy Measure of 3D Medical Image Alignment," *Pattern Recognition*, vol. 32, no. 1, pp. 71–86, Jan. 1999.

[11] Ken Shoemake and Tom Duff, "Matrix animation and polar decomposition," 1992, pp. 258–264.